Bulletin of Mathematical Biology (2019) 81:4932–4950
https://doi.org/10.1007/s11538-019-00665-2

Society for Mathematical Biology

ORIGINAL ARTICLE

Compensatory Foraging in Stoichiometric Producer–Grazer Models

Angela Peace[1] · **Hao Wang**[2]

Received: 18 April 2019 / Accepted: 10 September 2019 / Published online: 20 September 2019
© Society for Mathematical Biology 2019

Abstract
Nutritional constraints are common as food resources are rarely optimally suited for grazing species. Elemental mismatches between trophic levels can influence population growth and foraging behaviors. Grazing species, such as *Daphnia*, utilize optimal foraging techniques, such as compensatory feeding. Here, we develop two stoichiometric producer–grazer models, a base model that incorporates a fixed energetic foraging cost and an optimal foraging model where energetic foraging costs depend on food nutritional content. A variable energetic foraging cost results in cell quota-dependent predation behaviors. Analyzing and comparing these two models allows us to investigate the potential benefits of stoichiometric compensatory foraging behaviors on grazer populations. Optimal foraging strategies depend on environmental conditions, such as light and nutrient availability. In low-light conditions, fixed energetic foraging appears optimal regardless of the nutrient loads. However, in higher light conditions and intermediate nutrient loads, grazers utilizing compensatory foraging strategies gain an advantage. Overall, grazers can benefit from compensatory feeding behaviors when the food nutrient content of their prey becomes low or high.

Keywords Ecological stoichiometry · Predator–prey · Foraging strategies

1 Introduction

Optimal foraging theory employs models that aim to predict animal behaviors that maximize their fitness (Pyke et al. 1977). In many cases, the intake of energy or food quantity is used as a measure of fitness; however, maximizing energy intake does not always correlate to maximizing fitness. As organisms are composed of multiple chemical elements, foraging strategies also incorporate regulation of multiple nutrients

✉ Angela Peace
a.peace@ttu.edu

1 Department of Mathematics and Statistics, Texas Tech University, Lubbock, USA

2 Department of Mathematical and Statistical Sciences, University of Alberta, Edmonton, Canada

(Simpson et al. 2004). Elemental mismatches between grazers and their food resources can have significant consequences on their growth and reproduction (Sterner and Elser 2002). Ingesting nutritionally imbalanced diets leads to trade-offs between the costs of foraging efforts and filling nutrient deficits while also dealing with the ingestion of excess nutrients. There is growing evidence that animals employ foraging strategies based on the nutritional content of their food (Simpson et al. 2004). These foraging strategies depend on food quality rather than food quantity.

In order to investigate the effects of stoichiometry-dependent foraging strategies under nutrient constraints, we develop producer–grazer models under the framework of Ecological Stoichiometry (Sterner and Elser 2002). Models developed under the theory of Ecological Stoichiometry consider multiple chemical elements and their ratios across trophic levels, in order to incorporate food quantity and quality into a single framework. Andersen (1997) introduced stoichiometric effects into the classical Rosenzweig MacArthur equations with the incorporation of nutrient-deficient growth by modifying the density dependence of the producer's growth rate and the grazer's growth efficiency. Introduction of these stoichiometric constraints significantly affects the population dynamics and stability properties of the system Andersen (1997), Andersen et al. (2004). Following Andersen's approach, Loladze et al. (2000) formulated a producer–grazer model (LKE model) of the first two trophic levels of an aquatic food chain (algae-*Daphnia*) incorporating the fact that both producers and grazers are chemically heterogeneous organisms composed of two essential elements, carbon (C) and phosphorus (P). The model allows the phosphorus to carbon ratio (P:C) of the producer to vary above a minimum value. This variable P:C ratio of the producer brings food quality into the model.

Grazer ingestion rates of most stoichiometric models consider Holling type II functional responses (Holling 1965, 1966) that depend on producer quantity, but not quality (Loladze et al. 2000; Wang et al. 2008; Peace et al. 2013, 2014; Peace 2015). There are some complex computer simulations models that do consider stoichiometric foraging strategies (Darchambeau 2005; Mitra and Flynn 2007; Acheampong et al. 2014). These complex models consider varying ingestion, assimilation, and metabolism rates and efficiencies that depend on gut passage time (Darchambeau 2005; Mitra and Flynn 2007), and temperature (Acheampong et al. 2014). However, the complexities of these models are difficult to incorporate into dynamic population models.

Suzuki-Ohno et al. (2012) developed a simple model of compensatory feeding by incorporating optimal foraging rates into a grazer functional response as filter feeders *Daphnia* have limited ability to distinguish different food items and may benefit from compensatory feeding behaviors (Suzuki-Ohno et al. 2012). They describe a forager's growth rate in terms of carbon as a function of the prey density (x) with the following expression:

$$G(x) = (\alpha - \beta) f(x) - (\xi_B + \delta + \xi_f) \tag{1}$$

where α and β are the carbon (C) assimilation efficiency and cost of assimilation, respectively, ξ_B is the basal energetic cost for survivorship and δ is the biomass loss. Parameter ξ_f is the cost of feeding effort, which is the amount of C consumed a day to

generate energy necessary for feeding behaviors. The feeding rate $f(x)$ is represented as

$$f(x) = \frac{\mu\xi_f x}{1 + \mu\xi_f \tau x} \tag{2}$$

where $\mu\xi_f$ is the encounter rate with the prey and τ is the handling time. Suzuki-Ohno et al. (2012) describe μ as the amount of water per unit of C invested to generate energy for feeding behaviors and τ as the minimum amount of gut passage time for digestion. They use the above foraging behaviors in a simple steady-state model to show that optimal feeding rate increased by using excess C when the producer's relative P content was less than a critical level known as the threshold elemental ratio (TER). Additionally, they found that the TER depended on the producer's density. Here, we follow the approach utilized by Suzuki-Ohno et al. (2012) to describe stoichiometric foraging behavior and incorporate it into dynamic population models.

We first develop a base model by modifying the functional form of the grazer ingestion rate and incorporating a fixed energetic cost for foraging efforts to the stoichiometric producer–grazer model (WKL model) developed by Wang et al. (2008). We then develop an optimal foraging model where the energetic cost for foraging depends on producer nutritional composition parameterized with empirical data from Elser et al. (2016). Analyzing and comparing these two models allows us to investigate the potential benefits of stoichiometric compensatory foraging behaviors on grazer populations.

2 Model Formulation

We formulate models of the first two trophic levels of an aquatic food chain, with primary producer x (algae, mg C/L) and grazer y (*Daphnia*, mg C/L). It is well documented that the elemental composition of algae varies widely when compared to that of aquatic herbivores (Sterner and Elser 2002). Additionally, since *Daphnia* have high nutrient demands, they are often limited by the quantity of mineral elements in their food, rather than the amount of food or energy available (Sterner and Hessen 1994). In order to incorporate such stoichiometric constraints, we assume that the producer has a variable P:C ratio Q and the grazer has a constant P:C ratio θ. The amount of free P in the environment is explicitly tracked and denoted as resource R.

The models assume that the grazer has a Holling type II functional response and directly incorporate the carbon cost of feeding effort. First, we present a base model (Sect. 2.1) where foraging behavior depends on available producer quantity, then we develop an optimal foraging model (Sect. 2.2) where foraging behavior depends on available producer quantity and quality. Finally, we employ quasi-steady-state assumptions to reduce the models from four- to two-dimensional systems of ordinary differential equations (Sect. 2.3).

2.1 Base Model

The base model takes the following form:

$$\underbrace{\frac{\mathrm{d}x}{\mathrm{d}t}}_{\substack{\text{algae density}\\ \text{over time}}} = \underbrace{b \min\left\{1 - \frac{x}{K}, 1 - \frac{q}{Q}\right\} x}_{\substack{\text{gain from}\\ \text{growth}}} \quad \underbrace{-f(x)y}_{\substack{\text{loss from}\\ \text{predation}}} \tag{3a}$$

$$\underbrace{\frac{\mathrm{d}y}{\mathrm{d}t}}_{\substack{\textit{Daphnia}\text{ density}\\ \text{over time}}} = \underbrace{e \min\left\{1, \frac{Q}{\theta}\right\} f(x)y}_{\substack{\text{gain from}\\ \text{growth}}} \quad \underbrace{-\xi y}_{\substack{\text{C cost of}\\ \text{feeding effort}}} \quad \underbrace{-\delta y}_{\substack{\text{loss from}\\ \text{death}}} \tag{3b}$$

$$\underbrace{\frac{\mathrm{d}Q}{\mathrm{d}t}}_{\substack{\text{algal P:C}\\ \text{over time}}} = \underbrace{v(Q, R)}_{\substack{\text{uptake from}\\ \text{environment}}} \quad \underbrace{-b \min\left\{1 - \frac{x}{K}, 1 - \frac{q}{Q}\right\} Q}_{\substack{\text{loss due to}\\ \text{growth}}} \tag{3c}$$

$$\underbrace{\frac{dR}{\mathrm{d}t}}_{\substack{\text{free P}\\ \text{over time}}} = -\underbrace{v(Q, R)x}_{\substack{\text{algal}\\ \text{uptake}}} + \underbrace{\theta y(\delta + \xi)}_{\substack{\textit{Daphnia}\\ \text{loss}}} + \underbrace{\left(Q - e \min\left\{1, \frac{Q}{\theta}\right\} \theta\right) f(x)y}_{\substack{\textit{Daphnia}\\ \text{recycling}}} \tag{3d}$$

where b is the maximum producer growth rate, K is the producer carrying capacity in terms of light, q is the producer minimum P:C ratio needed for survival, e is the grazer maximum conversion efficiency, δ is the grazer loss rate, and ξ is the feeding cost.

Similar to previous models developed under the framework of Ecological Stoichiometry (Andersen et al. 2004; Loladze et al. 2000), our models employ nonsmooth minimum function in the growth rate expressions. The use of these functions follows from Justin Leibig's law of the minimum, which states that an organism's growth will be limited by whichever single resource is in the lowest supply relative to the organism's needs (Sterner and Elser 2002). Here, we assume the growth rates are limited either by C or P. This results in the minimum functions with two inputs seen in the expressions for growth in model (3).

The uptake of a resource depends on the amount of that resource available, as well as the amount of the resource that an organism currently has. Following Andersen (1997) and Diehl (2007a), we assume that algal P uptake is an increasing function of environmental nutrient concentration (R) and a decreasing function of internal nutrient stores (Q). This uptake function takes the following form:

$$v(Q, R) = \left[\frac{\hat{v}R}{\alpha + R}\right]\left[\frac{\hat{Q} - Q}{\hat{Q} - q}\right] \tag{4}$$

where $\hat{v}$ is the prey maximum P:C uptake rate and α is the P half saturation constant. The maximum algal P:C ratio is $\hat{Q}$, and its minimum P:C ratio is q. $f(x, Q)$ is the grazer's functional response, which depends on food quantity (x) and quality (Q).

Compensatory feeding can play an important role in maintaining herbivore populations as the quality of their food varies (Cruz-Rivera and Hay 2000). Here, we associate compensatory feeding into the functional response that incorporates a cost of feeding effort. First, we assume the grazer's ingestion rate, $f(x)$, a Holling type II functional response. Following Suzuki-Ohno et al. (2012), we assume the encounter rate with the producer increases linearly with feeding effort and $f(x)$ takes the following form:

$$f(x) = \frac{\mu \xi x}{1 + \mu \xi \tau x} \tag{5}$$

where ξ is the feeding effort, τ is the handling time, and μ is the amount of water cleared per mg C invested to generate energy for filtering behavior. The base model (3) is similar to the WKL model developed by Wang et al. (2008) with the addition of the grazer's feeding cost, ξ, and a modified functional response $f(x)$ given in Eq. (5).

While ξ is the C cost of the feeding effort, it is important to note our assumption that the *Daphnia* maintain a constant P:C ratio, θ. In order to maintain this homeostatic assumption, the *Daphnia* release P into the environment at a ratio proportional to this feeding effort, $\theta\xi$; see the second term in Eq. (3d).

2.2 Optimal Foraging Model

The optimal foraging model has the same structure as the base model (3) except that the grazer functional response $f(x)$ and the feeding effort ξ depend on food quality: $f(x, Q)$, $\xi(Q)$. The optimal foraging functional response can be written as

$$f(x, Q) = \frac{\mu \xi(Q) x}{1 + \mu \xi(Q) \tau x}. \tag{6}$$

Schatz and McCauley (2007) empirically investigated *Daphnia* foraging rates in spatial stoichiometric gradients of food quality (algal P:C ratios). They found that adult and juvenile *Daphnia* quickly locate regions of high-quality food and adjust their ingestion rates for algae of varying stoichiometric ratios. Their empirical data on *Daphnia* feeding behaviors, estimated from the depletion of algae densities over time, suggest that maximum ingestion rates decrease linearly with decreasing P:C ratio. However, Plath and Boersma (2001) monitored *Daphnia* feeding activity via measuring the beat rate of the filtering appendage and found that feeding activity decreases as algal P:C increases. These different results may be caused by different acclimation procedures as *Daphnia* acclimated under poor food quality will increase ingestion when given high-quality food (Schatz and McCauley 2007). Furthermore, Elser et al. (2016) found nonmonotonic responses of *Daphnia* ingestion rates to algal P:C by monitoring C^{14}-labeled algae in the grazer and the media. Here, we assume the feeding effort is quadratically related to food quality:

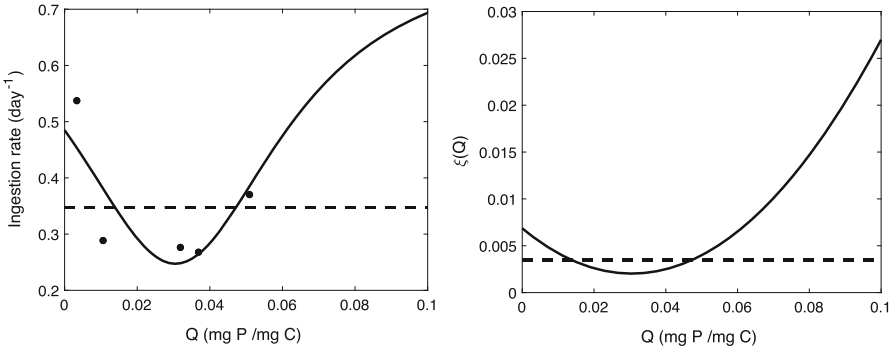

(a) Ingestion rate **(b)** Feeding costs

Fig. 1 Parameterization of *Daphnia* functional response for varying algal P:C ratios. Data (dots) from Elser et al. (2016) were used to fit Eq. (6) (solid curve) assuming $\xi(Q)$ can be described as the quadratic function given in Eq. (7). The data were also used to fit Eq. (5) assuming ξ is constant (dashed line). Parameter values obtained are listed in Table 1 with $x = 0.25$ mg C/L

$$\xi(Q) = a_1 Q^2 + a_2 Q + a_3 \tag{7}$$

and parameterize the optimal foraging functional response, Eq. (6) to the data for *Daphnia magna* (Elser et al. 2016). Figure 1 shows the data and functional response fits.

2.3 Model Reduction

The total amount of phosphorus in the system $P = R + Qx + \theta y$ is conserved, that is, $dP/\mathrm{d}t = dR/\mathrm{d}t + Q\mathrm{d}x/\mathrm{d}t + x\mathrm{d}Q/\mathrm{d}t + \theta \mathrm{d}y/\mathrm{d}t = 0$ according to the equations in model (3). The free nutrients can be expressed as

$$R = P - Qx - \theta y, \tag{8}$$

then the optimal foraging model can be reduced down to a system of three equations:

$$\underbrace{\frac{\mathrm{d}x}{\mathrm{d}t}}_{\substack{\text{algae density}\\ \text{over time}}} = \underbrace{b \min\left\{1 - \frac{x}{K}, 1 - \frac{q}{Q}\right\} x}_{\substack{\text{gain from}\\ \text{growth}}} \underbrace{-f(x, Q)y}_{\substack{\text{loss from}\\ \text{predation}}} \tag{9a}$$

$$\underbrace{\frac{\mathrm{d}y}{\mathrm{d}t}}_{\substack{\textit{Daphnia}\text{ density}\\ \text{over time}}} = \underbrace{e \min\left\{1, \frac{Q}{\theta}\right\} f(x, Q)y}_{\substack{\text{gain from}\\ \text{growth}}} \underbrace{-\xi(Q)y}_{\substack{\text{C cost of}\\ \text{feeding effort}}} \underbrace{-\delta y}_{\substack{\text{loss from}\\ \text{death}}} \tag{9b}$$

$$\underbrace{\frac{\mathrm{d}Q}{\mathrm{d}t}}_{\substack{\text{algal P:C}\\ \text{over time}}} = \underbrace{v(Q, P - Qx - \theta y)}_{\substack{\text{uptake from}\\ \text{environment}}} \underbrace{-b \min\left\{1 - \frac{x}{K}, 1 - \frac{q}{Q}\right\} Q}_{\substack{\text{loss due to}\\ \text{growth}}} \tag{9c}$$

Additional assumptions on the efficiency of the producer nutrient uptake can further reduce the models. Here, we assume the producer is extremely efficient at nutrient uptake and allow the maximum uptake to go to infinity $\hat{v} \to \infty$. Allowing $\hat{v} \to \infty$ removes the upper bound on the producer P:C ratio, $\hat{Q}$, and we allow $\hat{Q} \to \frac{P-\theta y}{x}$. The dynamics of the nutrients in the producer, Q, and the media, R, are much faster than the population growth dynamics of x and y. We apply quasi-steady-state assumptions on Eq. (9c) to obtain

$$Q = \begin{cases} \frac{\hat{v}R\hat{Q}}{\hat{v}R - b(1-\frac{x}{K})(\alpha+R)(\hat{Q}-q)} & \text{for } 1 - \frac{x}{K} < 1 - \frac{q}{Q} \\ \\ \frac{\hat{v}R\hat{Q} - q(\alpha+R)(\hat{Q}-q)}{\hat{v}R - b(\alpha+R)(\hat{Q}-q)} & \text{for } 1 - \frac{x}{K} > 1 - \frac{q}{Q} \end{cases}$$

where R is given by Eq. (8). For sufficiently fast nutrient processes, $\hat{v}$ is large. Taking $\hat{v} \to \infty$ in the above equation yields $Q \to \hat{Q} = \frac{P-\theta y}{x}$. Under these quasi-steady-state assumptions, the models can be reduced to two dimensions. The reduced base model takes the following form:

$$\underbrace{\frac{\mathrm{d}x}{\mathrm{d}t}}_{\substack{\text{algae density}\\ \text{over time}}} = \underbrace{b \min\left\{1 - \frac{x}{K}, 1 - \frac{q}{Q}\right\} x}_{\substack{\text{gain from}\\ \text{growth}}} \underbrace{- \frac{\mu\xi x}{1 + \mu\xi\tau x} y}_{\substack{\text{loss from}\\ \text{predation}}} \tag{10a}$$

$$\underbrace{\frac{\mathrm{d}y}{\mathrm{d}t}}_{\substack{\textit{Daphnia}\text{ density}\\ \text{over time}}} = \underbrace{e \min\left\{1, \frac{Q}{\theta}\right\} \frac{\mu\xi x}{1 + \mu\xi\tau x} y}_{\substack{\text{gain from}\\ \text{growth}}} \underbrace{-\xi y}_{\substack{\text{C cost of}\\ \text{feeding effort}}} \underbrace{-\delta y}_{\substack{\text{loss from}\\ \text{death}}} \tag{10b}$$

where

$$Q = \frac{P - \theta y}{x}, \tag{11}$$

and ξ is a constant. The reduced optimal foraging model takes the following form:

$$\underbrace{\frac{\mathrm{d}x}{\mathrm{d}t}}_{\substack{\text{algae density}\\ \text{over time}}} = \underbrace{b \min\left\{1 - \frac{x}{K}, 1 - \frac{q}{Q}\right\} x}_{\substack{\text{gain from}\\ \text{growth}}} \underbrace{- \frac{\mu\xi(Q) x}{1 + \mu\xi(Q)\tau x} y}_{\substack{\text{loss from}\\ \text{predation}}} \tag{12a}$$

$$\underbrace{\frac{\mathrm{d}y}{\mathrm{d}t}}_{\substack{\textit{Daphnia}\text{ density}\\ \text{over time}}} = \underbrace{e\min\left\{1, \frac{Q}{\theta}\right\}\frac{\mu\xi(Q)x}{1+\mu\xi(Q)\tau x}y}_{\substack{\text{gain from}\\ \text{growth}}} \underbrace{-\xi(Q)y}_{\substack{\text{C cost of}\\ \text{feeding effort}}} \underbrace{-\delta y}_{\substack{\text{loss from}\\ \text{death}}} \tag{12b}$$

where

$$Q = \frac{P-\theta y}{x} \qquad \text{and} \qquad \xi(Q) = a_1 Q^2 + a_2 Q + a_3. \tag{13}$$

3 Model Analysis

This section includes analysis of the reduced models [Systems (10) and (12)]. We determine the local stability of boundary equilibria, investigate the existence and stability of interior equilibria with a phase plane analysis, numerically observe periodic orbits, and conduct single- and two-parameter bifurcation analysis.

3.1 Boundary Equilibria

The boundary equilibria of the reduced models [Systems (10) and (12)] have the same form. There exists the trivial equilibrium $E_0 = (0, 0)$ with zero population densities. Additionally, there is a boundary equilibrium with grazer only extinction, $E_1 = (\min\{K, P/q\}, 0)$. In order to investigate the local stability of the boundary equilibrium, we first rewrite the base and optimal foraging models as follows:

$$\frac{\mathrm{d}x}{\mathrm{d}t} = xF(x, y) \tag{14a}$$

$$\frac{\mathrm{d}y}{\mathrm{d}t} = yG(x, y) \tag{14b}$$

where

$$F(x, y) = b\min\left\{1-\frac{x}{K}, 1-\frac{q}{Q}\right\} - \frac{\mu\xi}{1+\mu\xi\tau x}y \tag{15a}$$

$$G(x, y) = e\min\left\{1, \frac{Q}{\theta}\right\}\frac{\mu\xi x}{1+\mu\xi\tau x} - \xi - \delta \tag{15b}$$

for the base model (10), and

$$F(x, y) = b\min\left\{1-\frac{x}{K}, 1-\frac{q}{Q}\right\} - \frac{\mu\xi(Q)}{1+\mu\xi(Q)\tau x}y \tag{16a}$$

$$G(x, y) = e\min\left\{1, \frac{Q}{\theta}\right\}\frac{\mu\xi(Q)x}{1+\mu\xi(Q)\tau x} - \xi(Q) - \delta \tag{16b}$$

for the optimal foraging model (12). Then, the Jacobian can be written as

$$J = \begin{vmatrix} F(x, y) + xF_x(x, y) & xF_y(x, y) \\ yG_x(x, y) & G(x, y) + yG_y(x, y) \end{vmatrix}.$$

The Jacobian for both models evaluated at E_0 becomes

$$J(E_0) = \begin{vmatrix} b & 0 \\ 0 & G(0, 0) \end{vmatrix}.$$

Therefore, E_0 is unstable. The Jacobian for both models evaluated at E_1 becomes

$$J(E_1) = \begin{vmatrix} -b & * \\ 0 & G(\min\{K, P/q\}, 0) \end{vmatrix}.$$

The local stability of E_1 depends on the sign of $G(\min\{K, P/q\}, 0)$. If $G(\min\{K, P/q\}, 0) < 0$, then E_1 is a stable node, and if $G(\min\{K, P/q\}, 0) > 0$ then E_1 is an unstable saddle.

While the use of minimum functions is a convenient approach to incorporate stoichiometric constraints and allow organismal growth to be either limited by C or P, it does introduce nonsmooth functions into the models. These nonsmooth operators appear in elements of the Jacobian matrices. We note that these are derivatives of nondifferentiable functions. We utilize the Jacobian to show local stability of the boundary equilibria and verified the results via numerical simulations.

3.2 Interior Equilibria

Phase plane analyses for the reduced base model (10) for varying K values are presented in Fig. 2, and those for the reduced optimal foraging model (12) are in Fig. 3. We note that the nonsmooth minimum functions cause fragmentation to the phase plane and partitions parameter space, similar to previous works (Andersen et al. 2004; Loladze et al. 2000; Peace et al. 2013). Interior equilibria are located at the intersections of the producer and grazer nullclines. The stability of the interior equilibria was observed numerically and is denoted in Figs. 2 and 3 with solid (stable) and open (unstable) circles. The existence of periodic solutions was also observed numerically.

Under a low light intensity with $K = 0.25$ mg C/L, the base model has a stable interior equilibrium (Fig. 2a), whereas the optimal foraging model has a stable limit cycle (Fig. 3a). As the light intensity increases to $K = 0.75$ mg C/L, the base model exhibits a Hopf bifurcation and limit cycles emerge as the interior equilibrium loses its stability (Fig. 2b). Under this light intensity, the optimal foraging model exhibits a limit cycle with very large amplitude (Fig. 3b). As the light intensity further increases to $K = 1.25$ mg C/L, the base model has similar dynamics (Fig. 2c) but the limit cycles in the optimal foraging model collapse as two additional equilibria emerge, one stable and one unstable (Fig. 3c). The base model exhibits similar dynamics as the optimal foraging model at a higher light intensity with $K = 1.75$ mg C/L (Fig. 2d). Interestingly, for this very high level of light the optimal foraging model

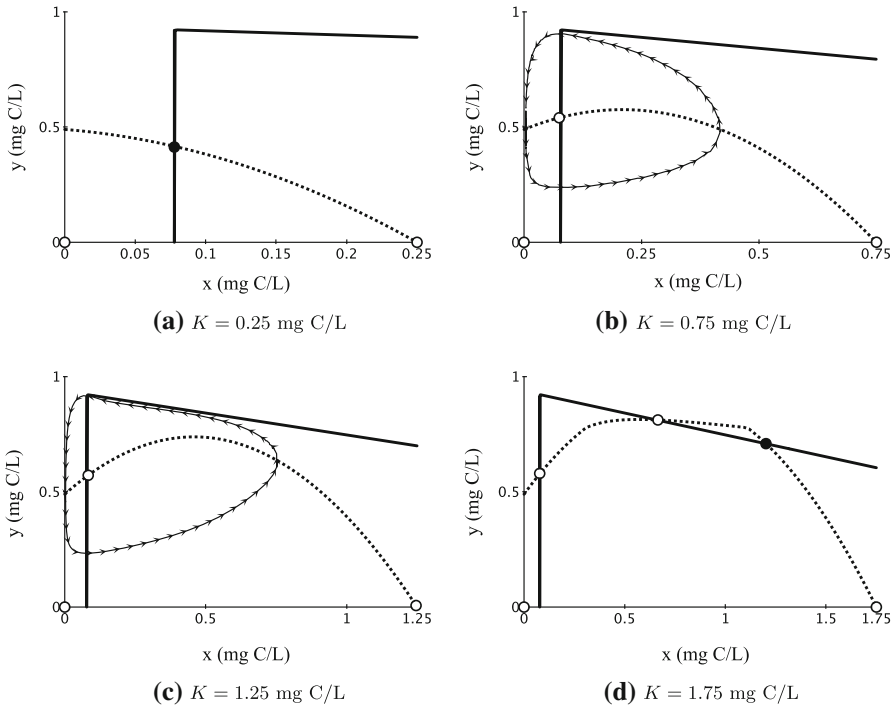

Fig. 2 Phase plane for the simplified base model for different light intensities. Dashed curves are producer nullclines, solid curves are grazer nullclines, solid circles are stable equilibria, open circles are unstable equilibria. Arrowed curves depict stable limit cycles solutions. Here, $P = 0.03$ mg P/L and all other parameter values are listed in Table 1

gains an additional two interior equilibria and exhibits bistability, with two stable interior equilibria (Fig. 3d).

3.3 Numerical Simulations

Figure 4 presents numerical simulations of the reduced base model (10) and optimal foraging model (12) that correspond to the phase planes depicted in Figs. 2 and 3. The ingestion rates for both models given in Eqs. (5) and (6) are shown in the last column.

3.4 Bifurcation Analysis

Here, we numerically conduct a bifurcation analysis using XPPAUT (Ermentrout 2002). The bifurcation diagrams are quite complicated, so we first present a bifurcation diagram of the well-studied LKE model by Loladze et al. (2000), shown in Fig. 5. For low K, the grazer is unable to survive due to low food quantity. As K increases, the grazer population increases. As K continues to increase, it reaches a Hopf bifurcation where limit cycles emerge. These limit cycles are abruptly halted

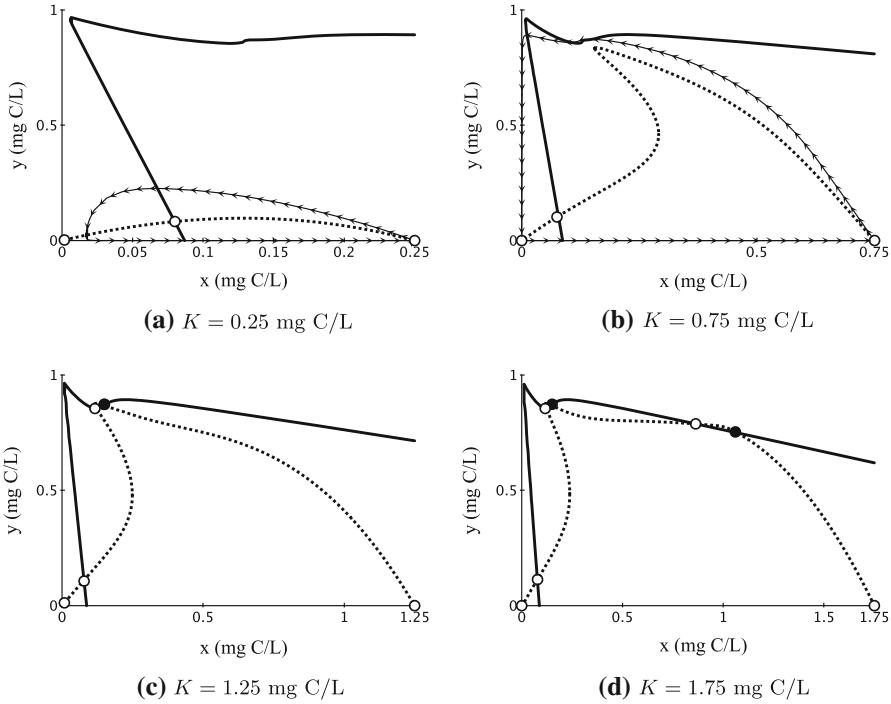

Fig. 3 Phase plane for the simplified optimal foraging model for different light intensities. Dashed curves are producer nullclines, solid curves are grazer nullclines, solid circles are stable equilibria, open circles are unstable equilibria. Arrowed curves depict stable limit cycles solutions

as K increases to a saddle-node bifurcation. After the saddle-node bifurcation, grazer densities start to decline and eventually reach extinction. High values of K result in low algal P:C ratio (Q), or low-quality food. The decline in grazer density is due to low food quality. More detailed bifurcation analyses of the LKE model have shown the model exhibits multiple regions of bistability as well (Li et al. 2011; Xie et al. 2018).

Similar to Loladze et al. (2000), we use nonsmooth minimum function to incorporate stoichiometric constraints and our bifurcation diagrams have a similar structure. Bifurcation diagrams of our reduced models, systems (10) and (12) are presented in Figs. 6, 7, 8, and 9 for different light intensities and P values.

For fixed intermediate $P = 0.03$ mg P/L, as shown in Fig. 6, under low light intensities the base model exhibits a stable coexistence equilibrium; however, the optimal foraging model exhibits periodic cycles with amplitudes that bring both populations near to extinction. Under these conditions, the *Daphnia* in the base model fair better than the optimal foraging model. As light increases, the base model exhibits a Hopf bifurcation and limit cycles emerge. There is a range of K where both models oscillate, but the cyclic amplitudes in the optimal foraging model remain larger. Eventually, for larger values of K the oscillations in the optimal foraging model disappear and a stable coexistence equilibrium emerges. This occurs at a saddle-node homoclinic connection

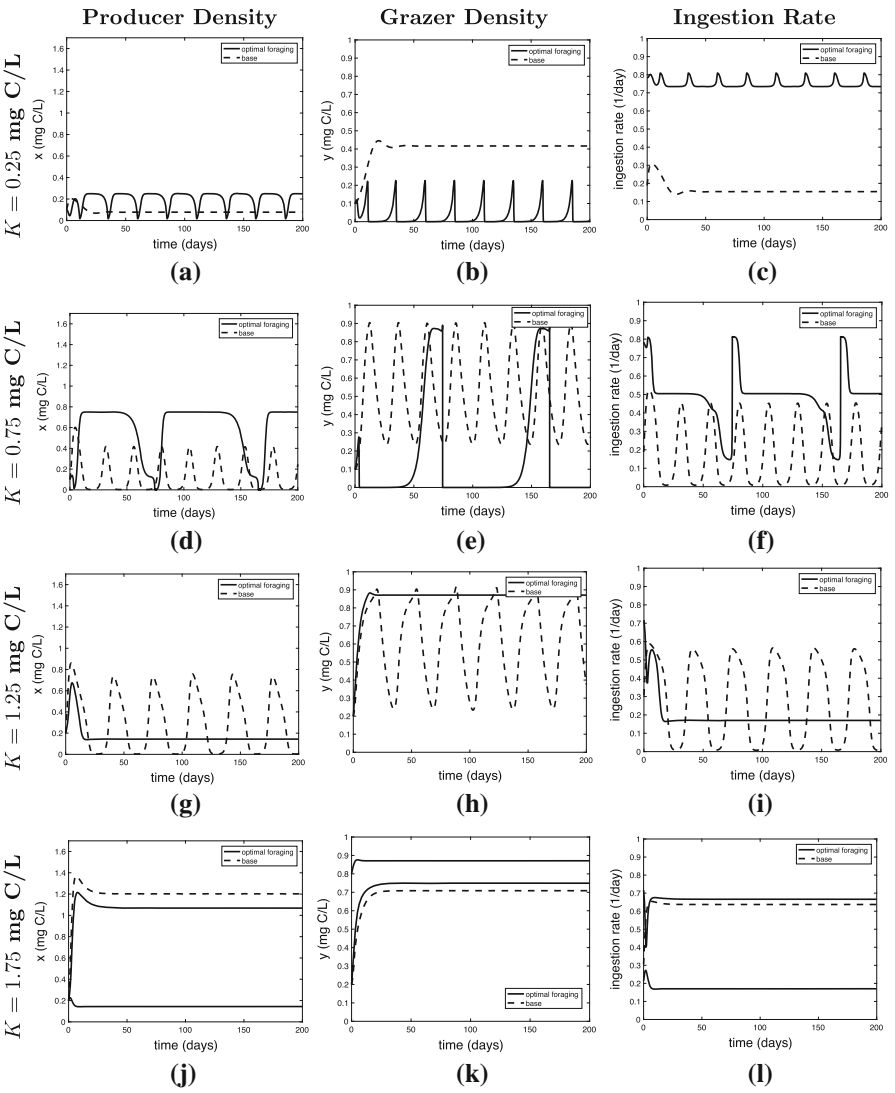

Fig. 4 Numerical simulations for the reduced base model (dashed) and optimal foraging model (solid) for population densities x, y C/L and grazer ingestion rates f for different light intensities: **a–c** $K = 0.25$ mg C/L, **d–f** $K = 0.75$ mg C/L, **g–i** $K = 1.25$ mg C/L, and **j–l** $K = 1.75$ mg C/L. Here, $P = 0.03$ mg P/L and all other parameter values are listed in Table 1. Under a very high light intensity with $K = 1.75$ mg C/L, the optimal foraging model exhibits bistability, and two solutions with different initial conditions are shown in **j–l**

(details of a similar bifurcation for the LKE model are presented in Van Voorn et al. (2010).

This is the turning point, where the optimal foraging behavior begins to benefit the *Daphnia*. Here, the base model predicts oscillatory dynamics, while optimal foraging behaviors allow the *Daphnia* to remain at high population densities. As K increases, the

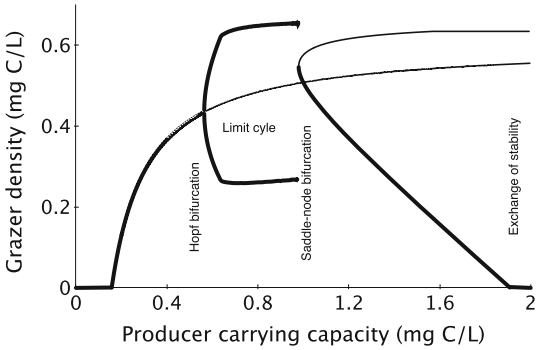

Fig. 5 Bifurcation diagram of the LKE model by Loladze et al. (2000) of the grazer population for varying light-dependent producer carrying capacity K. Thick lines are stable equilibria and extrema of stable limit cycles, and thin lines are unstable equilibria

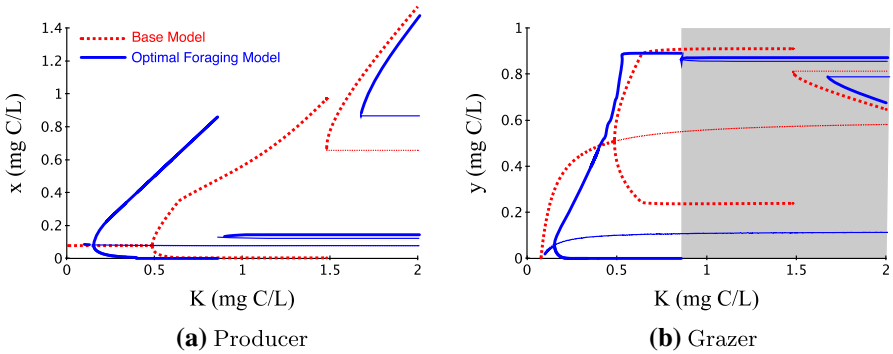

Fig. 6 Bifurcation diagrams for varying light-dependent carrying capacity K with intermediate nutrient level $P = 0.03$ mg P/L. All other parameter values are listed in Table 1. Dashed red curves are for the base model, and blue solid curves are for the optimal foraging model. Thick curves represent stable equilibria and the maximum and minimum of stable limit cycles. Thin curves are unstable branches. Optimal foraging behaviors benefit the grazers in the shaded region (Color figure online)

base model also goes through a saddle-node bifurcation as the cycles collapse to a stable equilibrium. Eventually, as light increases to very high values *Daphnia* populations begin to decline in the base models due to poor food quality. This is a well-observed phenomenon in stoichiometric producer–grazer models (Loladze et al. 2000; Wang et al. 2008; Peace 2015). Under these very high light intensities, the optimal foraging model exhibits bistability. One equilibrium at high *Daphnia* densities predating on a low quantity of very-high-quality algae, and another equilibrium with low *Daphnia* population densities, similar to the dynamics of the base model.

Figure 7 presents bifurcation diagram under a low nutrient level $P = 0.02$ mg P/L. Under low light intensities, the bifurcation dynamics are similar to Fig. 6; the base model has a stable equilibrium and the optimal foraging model has stable limit cycles. As light increases, The optimal foraging model exhibits the saddle-node bifurcation and its limit cycles collapse before the base model exhibits its Hopf bifurcation. Interestingly, the limit cycles emerging in the base model have smaller amplitudes than before and persist as light further increases. As light continues to increase, the base model becomes bistable with a small-amplitude stable limit cycle and a stable interior equilibrium.

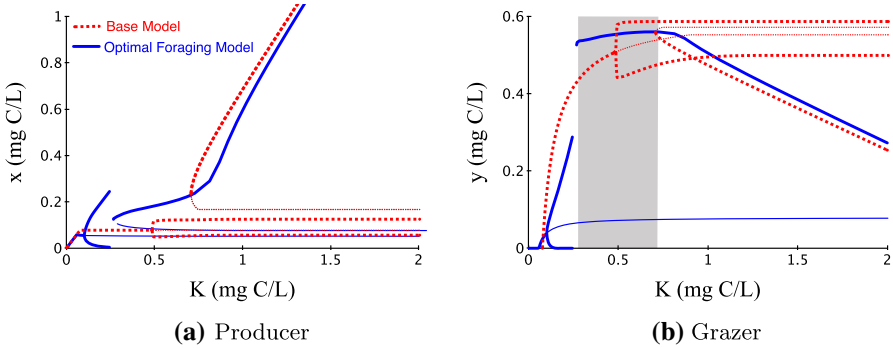

Fig. 7 Bifurcation diagrams for varying light-dependent carrying capacity K with low nutrient level $P = 0.02$ mg P/L. All other parameter values are listed in Table 1. Dashed red curves are for the base model, and blue solid curves are for the optimal foraging model. Thick curves represent stable equilibria and the maximum and minimum of stable limit cycles. Thin curves are unstable branches. Optimal foraging behaviors benefit the grazers in the shaded region (Color figure online)

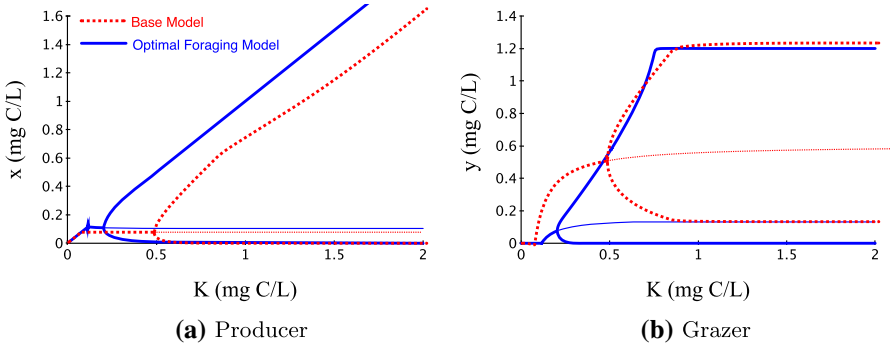

Fig. 8 Bifurcation diagrams for varying light-dependent carrying capacity K with high nutrient level $P = 0.04$ mg P/L. All other parameter values are listed in Table 1. Dashed red curves are for the base model, and blue solid curves are for the optimal foraging model. Thick curves represent stable equilibria and the maximum and minimum of stable limit cycles. Thin curves are unstable branches (Color figure online)

Figure 8 presents bifurcation diagram for a high nutrient level $P = 0.04$ mg P/L. Under low light intensities, this bifurcation diagram is similar to low and intermediate P conditions; however, as light increases the limit cycles of both models persist. The amplitudes of the limit cycles are large and the producer populations reach extremely low values (almost extinction). In the optimal foraging model, the large-amplitude limit cycles bring the grazer population densities near extinction as well.

A two-parameter bifurcation diagram for varying light level K and varying nutrient level P is presented in Fig. 9. The location of the Hopf and saddle-node bifurcations observed in the above one-dimensional bifurcation diagrams divides the parameter space into multiple regions. The colored regions in Fig. 9 are regions of oscillations. Outside these regions, both models have stable equilibria. The optimal foraging model exhibits limit cycles in blue region 1, the base model has limit cycles in red region 2, and both models cycle in purple region 3.

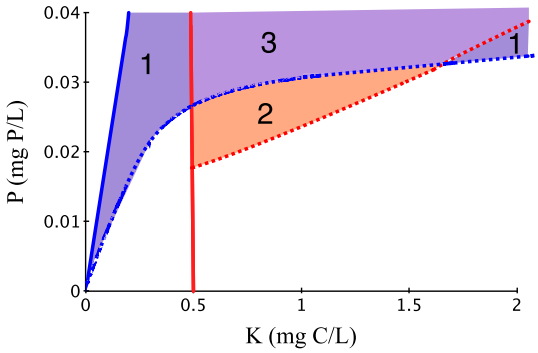

Fig. 9 A two-parameter bifurcation diagram for varying light level K and varying nutrient level P. All other parameter values are listed in Table 1. Red corresponds to the base model, and blue corresponds to the optimal foraging model. Solid red and blue curves depict Hopf bifurcations, and dashed red and blue curves depict saddle-node bifurcations. The optimal foraging model exhibits oscillations in region 1, the base model exhibits oscillations in region 2, and both models exhibit oscillations in region 3. Outside these regions, both models have stable equilibria (Color figure online)

4 Discussion

Optimal foraging behaviors of grazers depend on both food availability as well as stoichiometric constraints. The base model [System (3)] is a stoichiometric producer–grazer model that employs a Holling type II functional response which incorporates the carbon cost of feeding efforts as suggested by Suzuki-Ohno et al. (2012). The optimal foraging model (System (6)) expands the base model under the assumption that the feeding effort is quadratically related to food quality as observed empirically by Elser et al. (2016). Comparing the two models allows us to gain insight into the conditions where optimal foraging behaviors benefits the grazers.

Under intermediate P conditions and low–medium light intensities, the grazers in the base model appear to have an advantage of those in the optimal foraging model. The model simulations in Fig. 4b show the grazer population at stable values for the base model, whereas the population oscillates near extinction for the optimal foraging model. Under slightly higher light in Fig. 4e, both models predict oscillations in the grazer population; however, the larger amplitude oscillations in the optimal foraging model bring the population near extinction. For medium–high light intensities, the grazers in the optimal foraging model gain the advantage. Figure 4h shows the grazer population saturates to a high stable value for the optimal foraging model, whereas the population oscillates for the base model. Under high light intensities, both models predict that the grazer population saturates at high stable values, as shown in Fig. 4k, but it is higher in the optimal foraging model. Interestingly, the optimal foraging model exhibits bistability with two high-value stable equilibria.

These comparative dynamics of the two models can also be observed in the bifurcation diagrams. Regardless of P levels, under low light the grazer in the base model does better than that in the optimal foraging model. This can be observed from the left portion of the bifurcation diagrams Figs. 6, 7, and 8 where the base model has a stable equilibrium and the optimal foraging model has large-amplitude oscillations.

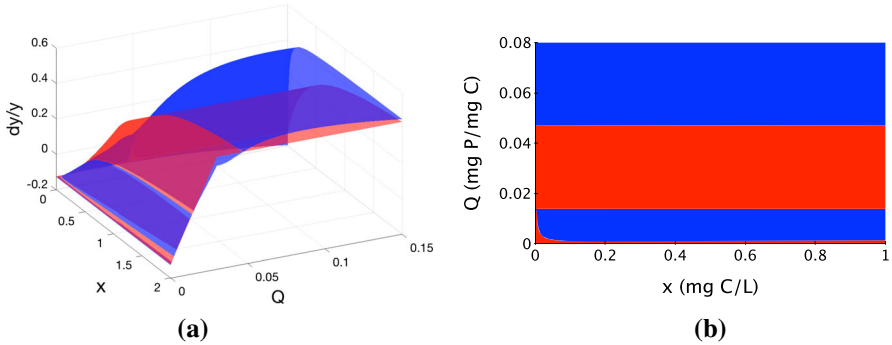

Fig. 10 **a** Per capital growth rates of the grazer population for the base model (red) and the optimal foraging model (blue) as functions of x and Q for the steady-state scenario in Eqs. (17) and (18). **b** Comparison of the two surfaces in $x - Q$ parameter space, grazer per capital growth rates are higher for the base model in the red regions and higher for the optimal foraging model in the blue regions (Color figure online)

Under intermediate levels of P, the grazer in the optimal foraging model gains the advantage for higher light intensities (shaded region of Fig. 6). A high grazer density stable equilibrium emerges in the optimal foraging model, and the base model exhibits oscillations. Under low P conditions, the grazer in the optimal foraging model only has the advantage for a small region of intermediate light intensities (shaded region of Fig. 7). The base model exhibits bistability with a stable equilibrium and a stable limit cycle. The stable equilibrium has similar dynamics as the one in the optimal foraging model for high light intensities. Under high P conditions, both models exhibit large-amplitude oscillations for high light intensities, although the low points of oscillations in the optimal foraging model get closer to extinction (Fig. 8). Arguably, the grazer in the base model has advantage in this scenario.

The observed bifurcation dynamics of nonsmooth stoichiometric models are rich. Robust analyses and global bifurcation have been conducted on the LKE model (Loladze et al. 2000). Li et al. (2011) performed a bifurcation analysis of the LKE model with Holling type II functional response with fixed parameter values and found the appearance of bistability. Xie et al. (2018) performed additional investigations with a complete global bifurcation without fixing any parameter. Here, they found multiple types of bistability. The global bifurcation analyses performed by Van Voorn et al. (2010) highlight the important ecological consequences of global bifurcations. We refer to these sources for details on robust bifurcation analyses to nonsmooth models and note that more rigorous analyses and global bifurcation on our models may shed more light into these dynamics and is left for future work.

Under the equilibrium case, we can visualize and compare the grazer per capita growth rates of the two models as functions of x and Q, by considering the grazer per capital growth rates for the base model:

$$\frac{\mathrm{d}y/\mathrm{d}t}{y} = e \min\left\{1, \frac{Q}{\theta}\right\} f(x) - \delta - \xi \tag{17}$$

Table 1 Model parameters

	Parameter	Value	Source
P	Total phosphorus	0.05 mg P/L	
K	Producer carrying capacity	0–4 mg C/L	
b	Maximal growth rate of producer	1.2/d	Andersen (1997), Urabe and Sterner (1996)
δ	Grazer loss rate	0.12/d	Suzuki-Ohno et al. (2012)
θ	Grazer constant P:C	0.03 mg P/mg C	Andersen (1997), Urabe and Sterner (1996)
q	Producer minimal P:C	0.0038 mg P/mg C	Andersen (1997), Urabe and Sterner (1996)
e	Maximal production efficiency	0.8 (unitless)	Andersen (1997), Urabe and Sterner (1996)
$\hat{v}$	Maximum P per C uptake rate of the producer	0.2 mg P/mg C/d	Diehl (2007b), Wang et al. (2008)
α	Phosphorus half saturation constant of the producer	0.008 mg P/L	Diehl (2007b), Wang et al. (2008)
$\hat{Q}$	Maximum quota	2.5 mg P/mg C	Andersen (1997)
μ	Water cleared/mg C invested to generate filtering energy	700 L/mg C	*
τ	Handling time ($\sim$ inverse of max feeding rate)	1.23 d	Suzuki-Ohno et al. (2012), Andersen (1997)
ξ	Feeding cost, constant for base model	0.0035 mgC/mgC/d	Elser et al. (2016) data fit (Fig. 1)
$\xi(Q)$	Feeding cost, function for optimal foraging model	$a_1 = 5.17$, $a_2 = -0.31$	Elser et al. (2016) data fit (Fig. 1)
	$\xi(Q) = a_1 Q^2 + a_2 Q + a_3$	$a_3 = 0.007$	

*There is no observational data available for parameter μ, amount of water cleared per unit of carbon invested to generate energy for filtering behavior. Suzuki-Ohno et al. (2012) used the arbitrary value of $\mu = 100$. Here, we used $\mu = 700$, which relates closer to the functional response used by Loladze et al. (2000)

and for the optimal foraging model:

$$\frac{\mathrm{d}y/\mathrm{d}t}{y} = e \min\left\{1, \frac{Q}{\theta}\right\} f(x, Q) - \delta - \xi(Q). \tag{18}$$

These surfaces are presented in Fig. 10 for varying x and Q values under the equilibrium case. The models suggest that the grazer can benefit from compensatory feeding behaviors for low and high food nutrient content (see the blue region in Fig. 10b). In many cases, the differences in height between the two surfaces in Fig. 10a are small, especially when the fitness of the base model (red) is higher than that of the optimal foraging model (blue). In these cases, the benefits of different foraging strategies may be small, especially considering any uncertainties in parameter values. The differences between the strategies are largest in scenarios of food low in quantity but high in P. We note that these surfaces are only showing dynamics at equilibria conditions, and bifurcation diagrams should be considered when the dynamics are oscillatory.

The models were parameterized with values from empirical observations, and several parameter values are used in previous studies, see Table 1. However, the lack of long-term datasets of population dynamics with corresponding measurements of varying stoichiometric ratios makes model validation challenging. While future datasets will help validate modeling efforts, the analyses presented here provide insight into the possible qualitative dynamics as light and P levels vary, rather than accurate quantitative predictions.

The developed models only consider one producer population, a single species of algae with a variable P:C ratio, and the optimal foraging model employs compensatory feeding behaviors. An alternative strategy for grazers to deal with stoichiometric constraints is to ingest a variety of prey of different elemental compositions. This strategy, called complementary feeding (Simpson et al. 2004; Suzuki-Ohno et al. 2012), includes a mixed diet composed of several producer species. A natural extension of the model presented here can include multiple producer populations.

Additionally, population dynamics can be more complicated with the consideration of spatial variation in food quality. Schatz and McCauley (2007) tested how *Daphnia* fair under a spatial gradient of algal P:C ratios while algal densities were held constant. *Daphnia* adjusted their ingestion rates and were able to quickly locate regions of high-quality food.

Acknowledgements The first author is partially supported by NSF grant DMS-1615697. The second author is partially supported by an NSERC grant. We would like to thank Alan Hastings for the initial discussion when the second author visited his laboratory in 2015.

References

Acheampong E, Hense I, John MAS (2014) A model for the description of feeding regulation by mesozooplankton under different conditions of temperature and prey nutritional status. Ecol Model 272:84–97

Andersen T (1997) Pelagic nutrient cycles: herbivores as sources and sinks. Springer-Verlag, New York

Andersen T, Elser JJ, Hessen DO (2004) Stoichiometry and population dynamics. Ecol Lett 7(9):884–900

Cruz-Rivera E, Hay ME (2000) Can quantity replace quality? Food choice, compensatory feeding, and fitness of marine mesograzers. Ecology 81(1):201–219

Darchambeau F (2005) Filtration and digestion responses of an elementally homeostatic consumer to changes in food quality: a predictive model. Oikos 111(2):322–336
Diehl S (2007a) Paradoxes of enrichment: effects of increased light versus nutrient supply on pelagic producer-grazer systems. Am Nat 169(6):E173–E191
Diehl S (2007b) Paradoxes of enrichment: effects of increased light versus nutrient supply on pelagic producer-grazer systems. Am Nat 169(6):E173–E191
Elser JJ, Kyle M, Learned J, McCrackin ML, Peace A, Steger L (2016) Life on the stoichiometric knife-edge: effects of high and low food c: P ratio on growth, feeding, and respiration in three daphnia species. Inland Waters 6(2):136–146
Ermentrout B (2002) Simulating, analyzing, and animating dynamical systems: a guide to XPPAUT for researchers and students, vol 14. SIAM, Philadelphia
Holling CS (1965) The functional response of predators to prey density and its role in mimicry and population regulation. Memoirs Entomol Soc Canada 97(S45):5–60
Holling CS (1966) The functional response of invertebrate predators to prey density. Memoirs Entomol Soc Canada 98(S48):5–86
Li X, Wang H, Kuang Y (2011) Global analysis of a stoichiometric producer–grazer model with holling type functional responses. J Math Biol 63(5):901–932
Loladze I, Kuang Y, Elser JJ (2000) Stoichiometry in producer-grazer systems: linking energy flow with element cycling. Bull Math Biol 62(6):1137–1162
Mitra A, Flynn KJ (2007) Importance of interactions between food quality, quantity, and gut transit time on consumer feeding, growth, and trophic dynamics. Am Nat 169(5):632–646
Peace A (2015) Effects of light, nutrients, and food chain length on trophic efficiencies in simple stoichiometric aquatic food chain models. Ecol Model 312:125–135
Peace A, Zhao Y, Loladze I, Elser JJ, Kuang Y (2013) A stoichiometric producer-grazer model incorporating the effects of excess food-nutrient content on consumer dynamics. Math Biosci 244(2):107–115
Peace A, Wang H, Kuang Y (2014) Dynamics of a producer-grazer model incorporating the effects of excess food nutrient content on grazer's growth. Bull Math Biol 76(9):2175–2197
Plath K, Boersma M (2001) Mineral limitation of zooplankton: stoichiometric constraints and optimal foraging. Ecology 82(5):1260–1269
Pyke GH, Pulliam HR, Charnov EL (1977) Optimal foraging: a selective review of theory and tests. Q Rev Biol 52(2):137–154
Schatz GS, McCauley E (2007) Foraging behavior by daphnia in stoichiometric gradients of food quality. Oecologia 153(4):1021–1030
Simpson SJ, Sibly RM, Lee KP, Behmer ST, Raubenheimer D (2004) Optimal foraging when regulating intake of multiple nutrients. Anim Behav 68(6):1299–1311
Sterner RW, Elser JJ (2002) Ecological stoichiometry: the biology of elements from molecules to the biosphere. Princeton University Press, Princeton
Sterner RW, Hessen DO (1994) Algal nutrient limitation and the nutrition of aquatic herbivores. Annu Rev Ecol Syst 25(1):1–29
Suzuki-Ohno Y, Kawata M, Urabe J (2012) Optimal feeding under stoichiometric constraints: a model of compensatory feeding with functional response. Oikos 121(4):569–578
Urabe J, Sterner RW (1996) Regulation of herbivore growth by the balance of light and nutrients. Proc Nat Acad Sci 93(16):8465–8469
Van Voorn GA, Kooi BW, Boer MP (2010) Ecological consequences of global bifurcations in some food chain models. Math Biosci 226(2):120–133
Wang H, Kuang Y, Loladze I (2008) Dynamics of a mechanistically derived stoichiometric producer-grazer model. J Biol Dyn 2(3):286–296
Xie T, Yang X, Li X, Wang H (2018) Complete global and bifurcation analysis of a stoichiometric predator-prey model. J Dyn Diff Equat 30(2):447–472

Publisher's Note Springer Nature remains neutral with regard to jurisdictional claims in published maps and institutional affiliations.